Astron. Nachr. / AN **332**, No. 9/10, 1008 – 1011 (2011) / **DOI** 10.1002/asna.201111595

Line profile variability and magnetic fields of Wolf-Rayet stars: WR 135 and WR 136

A.F. Kholtygin[1,⋆], **S.N. Fabrika**[2], **N. Rusomarov**[1], **W.-R. Hamann**[3], **D.O. Kudryavtsev**[2], **L.M. Oskinova**[3], and **G.A. Chountonov**[2]

[1] Astrophysical Institute of Saint-Petersburg University, Russia
[2] Special Astrophysical Observatory, Russia
[3] Institute for Physics and Astronomy, University Potsdam, Germany

Received 2011 Sep 20, accepted 2011 Sep 26
Published online 2011 Dec 12

Key words stars: atmospheres – stars: magnetic fields – stars: winds – stars: Wolf-Rayet – techniques: polarimetric

We have obtained spectropolarimetric observations of two Wolf-Rayet stars, WR 135 (WC8) and W R136 (WN6), with the 6-m Russian telescope in July 2009 and July 2010. We have studied the He II 5412 Å line region, which contains also the C IV 5469 Å line (for WR 135 only). Our goals were to investigate the rapid line-profile variability (LPV) in WR star spectra and to search for magnetic fields. We find small amplitude emission peaks moving from the center of He II line to its wings during the night in spectra of both stars. These emission peaks are likely a signature of accelerating clumps in the stellar wind. We obtained upper limits of the magnetic field strength: ≈200 G for WR 135 and ≈50 G for WR 136.

1 Introduction

Massive OB stars are believed to be the progenitors of Wolf-Rayet (WR) stars. The expanding atmospheres (winds) of WR stars are supposed to be strongly clumped. Signatures of wind clumping mainly come from indirect observational evidence. These include the unusual ionization structure of the wind (Antokhin et. al. 1988), the IR emission-line ratios (Nugis & Niedzielski 1995), stochastic variations in the polarized light (Robert & Moffat 1989), the continuum excess in the IR, and the radio free-free emission (Runacres & Blomme 1996). Sometimes, more direct evidences are also found (e.g. Lepine et al. 1999).

Many of the OB stars, the progenitors of WR stars, are magnetic (Hubrig et al. 2006; Hubrig et al. 2011; Bychkov et al. 2009). Neutron stars, which are the final product of the WR-star evolution, have super-strong magnetic fields. Thus, it is reasonable to assume that the WR stars are also magnetic. Nevertheless, up to date, for no WR star a magnetic field has been detected.

A first attempt to find a magnetic field was made by Eversberg et al. (1999) for the brightest WR star γ^2 Velorum (WR 11, HD 68273). The fluxes for all Stokes parameters were measured in the wavelength interval 5200–6000 Å. No obvious circular line polarization features were seen across any emission line above the $3\sigma \sim 0.03\%$ instrumental level. An upper limit on the net effective magnetic field in the WR wind was estimated as $B \leq 280$ G.

The next attempt to detect a magnetic field for γ^2 Velorum was reported in 2002 by Chesneau & Moffat (2002). They used the échelle-spectropolarimeter CASPEC at the ESO 3.6-m telescope. For all studied emission lines no signal in the Stokes parameter V was detected.

St-Louis et al. (2008) have tried to detect the magnetic field for the single star WR 6. Spectra were obtained in December 2005 at CFHT with the spectropolarimeter Espadons ($R \sim 68\,000$) at the wavelength interval 3700–10500 Å. The authors have estimated an upper limit of the Stokes parameter $V \leq 0.005\,\%$ from the analysis the He II $\lambda\,4686$ Å line, which gives the upper limit $B \leq 25$ G. These upper limits are based on estimating the contribution of the conversion of the linear polarization into circular polarization and seems to be very uncertain.

In the present paper we outline the results of our observations of the two Wolf-Rayet stars WR 135 and WR 136.

2 Objects and observations

We selected two objects: WR 135 and WR 136, which are the brightest northern-sky WR-stars. We observed these stars with the 6-m telescopes of the Special Astrophysical Observatory, (SAO) Russia. In Table 1 we list the parameters of our targets.

The spectropolarimetric observations of both WR 135 and WR 136 were obtained during 3 nights in July 2009 and 2 nights in July 2010. All observations were done using the long slit spectrograph MSS (Main Stellar Spectrograph) located at the Nasmyth focus of the 6-m telescope, equipped with the polarization analyzer (Chountonov 2004). For the present observations we selected the wavelength interval $5220\,\text{Å} \leq \lambda \leq 5586\,\text{Å}$, that includes the strong emission

⋆ Corresponding author: afkholtygin@gmail.com

Table 1 Parameters of the stars.

Parameter	WR135	Ref.	WR136	Ref.
m_V (mag)	8.11	a	7.48	a
Spect. Class.	WC8	a	WN6	a
d (kpc)	1.74	b	1.8	b
$T_{\rm eff}$ (K)	6.3×10^4	c	5.5×10^4	d
$R_*/R_\odot$	2.6	c	6.4	d
$\log(L/L_\odot)$	5.3	c	5.5	d
$M_*/M_\odot$	9	e	10	f
$\log \dot{M}_*$ ($M_\odot$ yr^{-1})	–4.1	c	–3.8	d
V_∞ (km s^{-1})	1300	c	1700	d

[a]SIMBAD data base, [b]van der Hucht 2001,
[c]Koesterke & Hamann 1995, [d]Dessart et al. 2000,
[e]Hamann et al. 1993, [f]Hamann et al. 1994

Table 2 Journal of observations.

WR 135			WR 136		
Date	N	T	Date	N	T
2009 Jul 3	9	4:40	2009 Jul 1	24	6:52
2009 Jul 7	14	3:51	2010 Jul 25	22	5:28
			2010 Jul 26	16	3:51
Total	23	8:31	Total	62	16:11

Notes: N is the number of observations per night, T is the total time interval covered (hr:min). Exposure time was 15 min for WR 135 and 10/15 min for WR 136 in 2009 and 15 minutes for WR 136 in 2010.

line He II $\lambda\,5412$ Å, the marginal line O V $\lambda\,5471$ Å, and also some more weak lines.

A journal of the observations is given in Table 2. Flat-fielding, bias subtraction and wavelength calibration with ThAr lamp were done following the routine procedure using the MIDAS packet. For the best reliability of the Stokes parameter V we used two successive spectra of the same star with two opposite positions of the polarization analyzer.

The lines in the spectra of both WR 135 and WR 136 are very broad. Even small differences between the L and the R continuum slope may result in a notable polarization in such broad lines. For this reason we took a special care to have the same continuum shape and normalization in the L and R spectra.

3 Line profile microvariability and smTVS spectra

Both WR 135 and WR 136 shows strong LPVs. The dynamical spectra of the LPVs for WR 136 are presented in Figs. 1 and Figs. 2 (top panels).

The resulting dynamical spectra reveal spectral features that systematically move from a region near the line center toward the line edges. This pattern of line-profile variability is quite typical for WR stars (e.g. Lepine et al. 1999). The moving details in the dynamical LPV spectra are usually explained as being due the clumps moving outward in the wind. The amount of moving spectral features ($\sim$ tens) is much smaller than the estimated number of clumps in the wind ($\sim$ thousands, Antokhin et. al. 1988). This can be explained if the emission subpeaks are the combined signature of clusters of many clumps (Lepine et al. 1999; Kudryashova & Kholtygin 2001).

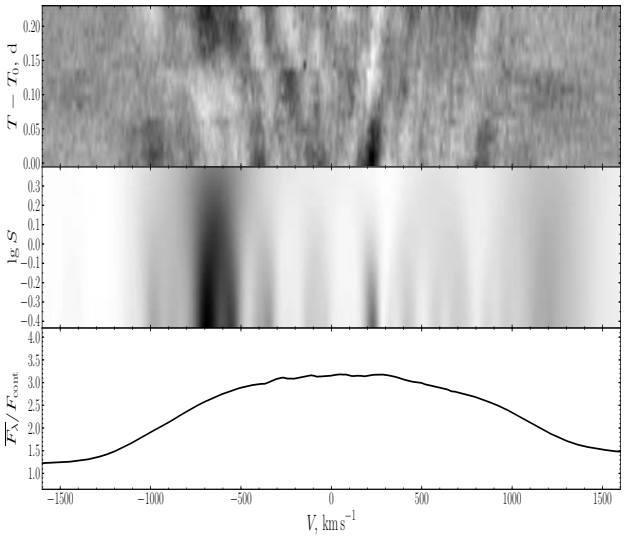

Fig. 1 *Top*: dynamical LPV for the line He II $\lambda\,5412$ in the spectra of WR 136 taken at July 25/26. *Middle*: grey scale dynamical plot of the smTVS spectrum as a function of the filter width S. *Bottom*: Nightly mean He II $\lambda\,5412$ line profile.

To detect the LPV of a small amplitude (micro-LPV) we use the smooth Time Variation Spectra (smTVS) technique introduced by Kholtygin et al. (2006). The value of $\mathrm{smTVS}(\lambda, \mathrm{S})$ is described by

$$\mathrm{smTVS}(\lambda, S) = \frac{1}{N-1} \times \left(\sum_{j=1}^{N} g_i \left[F_i(\lambda, S) - \overline{F(\lambda, S)} \right] \Big/ \sum_{j=1}^{N} g_j \right), \quad (1)$$

where N is number of spectra, $F(\lambda, S)$ is the flux in the spectrum with number i at wavelength λ smoothed with a Gaussian filter (S is the filter width) and normalized to the continuum, $\overline{F_j(\lambda, S)}$ is the flux at wavelength λ averaged over all smoothed fluxes, g_i is the relative weight of j-th observation. For $S = 0$, the value of $\mathrm{smTVS}(\lambda, S)$ corresponds to the $\mathrm{TVS}(\lambda, S)$ value introduced by Fullerton et al. (1996).

To ensure that the LPVs are real it is necessary to use a small significance level $\alpha \ll 1$ for the hypothesis that the line profile variations are due to random variations of the noise component of the profiles. In this case the smTVS value obeys a $\chi^2/(N-1)$ statistics with $N-1$ degrees of freedom. If the value of χ^2_α is specified, the probability becomes $P\left(\chi^2/(N-1) > \chi^2_\alpha\right) = \alpha$. Consequently, the hypothesis that the line profile is variable can be accepted if the calculated $\mathrm{smTVS}(\lambda)$ value exceeds χ^2_α.

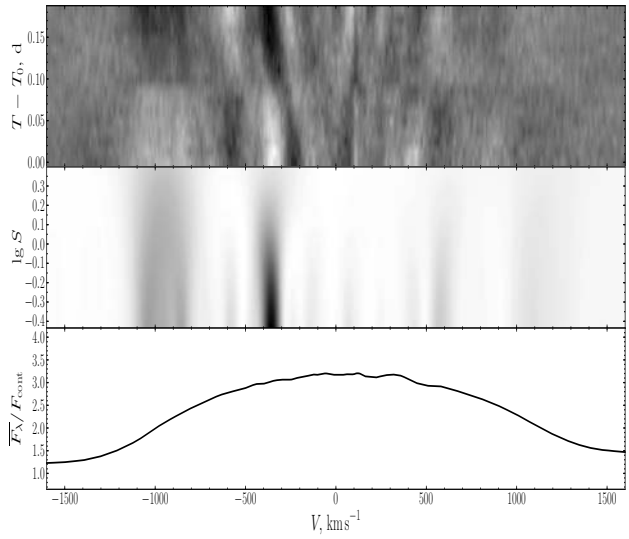

Fig. 2 The same as in Fig. 1, but for the night of July 26/27.

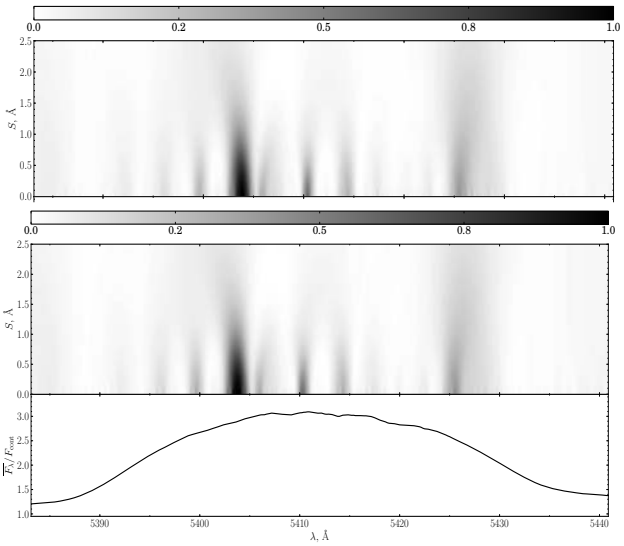

Fig. 3 *Top*: grey scale dynamical plot of the smTVS$_{\rm L}$ spectrum of the line He II λ 5412 for WR 136, obtained on 2009 July 1/2 as a function of the filter width S. *Middle*: the same as in top panel, but for smTVS$_{\rm R}$ spectrum. *Bottom*: nightly mean He II λ 5412 line profile.

It was shown empirically that the best results can obtained for smoothing with a Gaussian filter width S = 0.7–1.3 Å (it means usually 15–30 pixels). To illustrate our method, the smTVS map for the line He II $\lambda\,5412$ Å in spectra of WR 136 is plotted in Figs. 1 and 2 (middle panels) for the filter width $S \in (0.4\,\text{Å}, 2.5\,\text{Å})$.

As we can see in Figs. 1 and 2, the regions of the maximal amplitude on the smTVS map correspond to the moving bumps in the dynamical spectra of LPV. It means that smTVS spectra can be used for detecting stochastic line profile variations of small amplitudes.

4 Polarimetric line profile variability and the magnetic field

In our observations, besides the integral line profile intensity $I(\lambda)$ we obtained both polarization components of the line profile: the L component $I_{\rm L}^{\rm up}(\lambda)$ and R component $I_{\rm R}^{\rm up}(\lambda)$ for the "up" position of the polarization analyzer, and the corresponding values $I_{\rm L}^{\rm down}(\lambda)$, $I_{\rm R}^{\rm down}(\lambda)$ for the "down" position. In the first case, at the "up" position of the analyzer, the L and R components of the line are located at the top and the bottom of the CCD frame, respectively. At the "down" positions the L and R components are interchanged.

To find the corrected values of the left $I_{\rm L}(\lambda)$ and the right $I_{\rm R}(\lambda)$ components of the line profile we use the relation

$$\begin{cases} I_{\rm L}(\lambda) \;=\; [I_{\rm L}^{\rm up}(\lambda) \;+\; I_{\rm L}^{\rm down}(\lambda)]/2\,, \\ I_{\rm R}(\lambda) \;=\; [I_{\rm R}^{\rm up}(\lambda) \;+\; I_{\rm R}^{\rm down}(\lambda)]/2\,. \end{cases} \qquad (2)$$

In this case we use the same regions of the CCD matrix to find both $I_{\rm L}(\lambda)$ and $I_{\rm R}(\lambda)$ components and eliminate the errors connected with the inhomogeneous sensibility of CCD.

Applying Eq. (1) to the left polarized components $I_{\rm L}(\lambda)$ of the line we obtain the smTVS$_{\rm L}$ spectra. On the other hand, we obtain the smTVS$_{\rm R}$ spectra in the case of using the right polarized components $I_{\rm R}(\lambda)$. The density plot of the smTVS$_{\rm L}$ and smTVS$_{\rm R}$ for the line He II λ 5412 in spectra of WR 136, obtained during the night 2009 July 1/2 is shown in Fig. 3.

Darker areas correspond to the higher amplitudes in the smTVS$_{\rm L}$ and smTVS$_{\rm R}$ spectra. As can be seen from Fig. 3, the smTVS$_{\rm L}$ and smTVS$_{\rm R}$ spectra for WR 136 look nearly identical. Our calculatins show that in case of WR 135, the smTVS$_{\rm L}$ spectrum also looks the same as the smTVS$_{\rm R}$ one.

This finding means that the value of the global magnetic field for both stars cannot be large. We have estimated the Stokes parameter V for WR 135 and WR 136 in all our spectra. We obtain upper limits of the magnetic field strength as $\approx$200 G for WR 135 and $\approx$50 G for WR 136. The detailed description of the magnetic field measurements will be presented in a forthcoming paper (Kholtygin et al., in prep.)

5 Conclusions

From our spectropolarimetric observations of WR 135 and WR 136 we conclude that:

1. Our high accuracy polarimetric observations of WR 135 and WR 136 demonstrate the stochastic LPVs for both stars. The pattern of LPVs is in an accordance with the clumping stellar wind model.
2. On the smTVS map strong details connected with the stochastic structure of the wind are clearly seen. On the other hand, the difference between polarimetric maps smTVS$_{\rm L}$ and smTVS$_{\rm R}$ was not detected at all scales S.
3. The upper limits on the effective magnetic fields $B_{\rm e}$ both for WR 135 and WR 136 have been established. For WR 135 $B_{\rm e} \leq$ 200 G, but for WR 136 $B_{\rm e} \leq$ 50 G.

Acknowledgements. A.F.K. is grateful for the support provided by a Saint-Petersburg University project 6.38.73.2011. S.N.F. and D.O.K. thank for a support from the Scientific Leading Schools grant N 5473.2010.2.

References

Antokhin, I.I., Kholtygin, A.F., Cherepashchuk, A.M.: 1988, AZh 65, 558
Braithwaite, J., Nordlund, A.: 2006, A&A 450, 1077
Bychkov, V.D., Bychkova, L.V., Madej, J.: 2009, MNRAS 394, 1338
Chesneau, O., Moffat, A.F.J.: 2002, PASP 114, 612
Chountonov, G.A.: 2004, in: Y.V. Glagolevskij, O.I. Kudryavtsev, I.I.Romanyuk (eds.), *Magnetic Stars*, p. 286
Dessart, L., Crowther, P.A., Hillier, D.J., et al.: 2000, MNRAS 315, 407
Eversberg, T., Moffat, A.F.J., Marchenko, S.V.: 1999, PASP 111, 861
Fullerton, A.W., Gies, D.R., Bolton, C.T.: 1996, ApJS 103, 475
Hamann, W.-R., Koesterke, L., Wessolowski, U.: 1993, A&A 274, 397
Hamann, W.-R., Wessolowski, U., Koesterke, L.: 1994, A&A, 281, 184
Hamann, W.-R., Grafener, G., Liermann, A.: 2006, A&A 457, 1015
Hubrig, S., North, P., Schöller, M., Mathys, G.: 2006, AN 327, 289
Hubrig, S., Schöller, M., Kharchenko, N.V., et al.: 2011, A&A 528, A151
van der Hucht, K.A.: 2001, New A Rev. 45, 135
Kholtygin, A.F., Burlakova, T.E., Fabrika, S.N., et al.: 2006, Astron. Rep. 50, 887
Kholtygin, A.F., Chuntonov, G.A., Fabrika, S.N., et al.: 2007, in: I.I. Romanyuk, D.O. Kudryavtsev (eds.), *Physics of Magnetic Stars*, p. 262
Koesterke, L., Hamann, W.-R, 1995, A&A 299, 503
Kudryashova, N.A., Kholtygin, A.F.: 2001, Astron. Rep. 45, 287
Lepine, S., Eversberg, T., Moffat, A.F.J.: 1999, ApJ 117, 1441
MacGregor, K.B., Cassinelli, J.P.: 2003, ApJ 586, 480
Mestel, L.: 2003, in: L.A. Balona, H.F. Henrichs, R. Medupe (eds.), *Magnetic Fields in O, B and A Stars: Origin and Connection to Pulsation, Rotation and Mass Loss*, ASPC 305, p. 3
Moss, D.: 2001, in: G. Mathys, S.K. Solanki, D.T. Wickramasinghe (eds.), *Magnetic Fields Across the Hertzsprung-Russell Diagram*, ASPC 248, p. 305
Nugis, T., Niedzielski, A.: 1995, A&A 300, 237
Robert, C., Moffat, A.F.J.: 1989, ApJ 347, 1034
Runacres, M.C., Blomme, R.: 1996, in: J.M. Vreux, A. Detal, D. Fraipont-Caro, E. Gosset, G. Rauw (eds.), *Wolf-Rayet Stars in the Framework of Stellar Evolution*, p. 317
St-Louis, N., Chené, A.N., de La Chevrotière, A., Moffat, A.F.J.: 2008, in: A. de Koter, L. Smith, R. Waters (eds.), *Mass Loss from Stars and the Evolution of Stellar Clusters*, ASPC 388, p. 79